Optical and structural properties of ternary nanoaggregates in CsI-PbI_2 co-evaporated thin films

2000 J. Phys.: Condens. Matter 12 1939

(http://iopscience.iop.org/0953-8984/12/8/335)

J. Phys.: Condens. Matter **12** (2000) 1939–1946. Printed in the UK PII: S0953-8984(00)06352-9

Optical and structural properties of ternary nanoaggregates in $CsI–PbI_2$ co-evaporated thin films

M Nikl†*, K Nitsch†, J Chval†, F Somma‡, A R Phani§, S Santucci§, C Giampaolo‖, P Fabeni¶, G P Pazzi¶ and X Q Feng+

† Institute of Physics AS CR, Cukrovarnicka 10, 162 53 Prague, Czech Republic
‡ INFM and Department of Physics, University Roma Tre, via V Navale 84, 00146 Rome, Italy
§ INFM and Department of Physics, University of L'Aquila, via Vetoio 10, 67010 Aquila, Italy
‖ Department of Geology, University Roma Tre, Largo San L Murialdo 1, 00146 Rome, Italy
¶ IROE del CNR, via Panciatichi 64, 50 127 Florence, Italy
+ LFIM, Shanghai Institute of Ceramics, Ding Xi Road 1295, 200050 Shanghai, China

E-mail: nikl@fzu.cz

Received 26 July 1999, in final form 22 November 1999

Abstract. Thin films were grown by vacuum co-evaporation of CsI and PbI_2 compounds from two independent crucibles. X-ray diffraction spectroscopy revealed formation of $CsPbI_3$ and Cs_4PbI_6 nanoaggregates in the thin film samples and gave an estimate of their volume percentage as well. It provided also the grain size estimates, which were compared with direct observation of a thin film surface by atomic force microscopy. The absorption, luminescence and decay kinetics characteristics of thin films grown were measured. The optical characteristics of the mentioned ternary nanoaggregates were determined and compared with those of $CsPbX_3$ and Cs_4PbX_6 (X = Cl, Br) bulk structures.

1. Introduction

Optical properties of the ternary Cs–Pb–X (X = Cl, Br, I) compounds were investigated mainly in the case of $CsPbCl_3$ single crystals, namely reflection, excitation and luminescence spectra [1–3], Raman and infrared spectra [4, 5] and the band structure was calculated as well [6]. [6] shows also the absorption spectra of $CsPbX_3$ (X = Cl, Br) thin films. The creation of $CsPbCl_3$ nanocrystals in Pb-doped CsCl crystals was found and a quantum size effect in their luminescence was noticed [7]. The growth technology [8] and the luminescence including the decay kinetics model [9] has been reported in the literature for another ternary compound, namely the Cs_4PbCl_6 one. A close similarity with the emission properties of KCl:Pb was noticed. The ternary compounds based on X = Br are somewhat less investigated; the absorption and luminescence spectra of $CsPbBr_3$ were reported for the single crystal and thin film systems [10]. Similar formation of $CsPbBr_3$ nanocrystals in CsBr:Pb single crystals was evidenced as in the case mentioned of CsCl:Pb and the quantum size effect was invoked to explain the high temperature shift and broadening in their absorption and emission spectra with decreasing crystallite size [11–13]. The first results dealing with absorption, luminescence and decay kinetics of Cs_4PbBr_6 single crystals were also reported [12, 14]. Close similarity with the emission of KBr:Pb was noticed again. To our knowledge, there is only one study related to

* Corresponding author.

the $CsPbI_3$ crystals in the literature [15], namely their luminescence and reflection spectra are reported. Nothing is known about the optical properties of the Cs_4PbI_6 structure, even though its existence was proved in the CsI–PbI_2 phase diagram study [16]. The Cs_4PbX_6 (X = Cl, Br, I) compounds offer an interesting comparison with the classical model systems KX:Pb^{2+} (X = Cl, Br, I) for their luminescence and decay kinetics properties due to the same local structure of the emission centres themselves (octahedron $(PbX_6)^{4-}$) in both material groups, while their crystalline structures are generally different, namely trigonal and face centred cubic, respectively. In the detailed KX:Pb^{2+} luminescence kinetics study, interesting departures from the exponential decay of the slow component were noticed [17], which increase with the anion mass. A theoretical model dealing with this phenomenon has been reported recently, which is based on slow (ms time scale) relaxation of the surrounding crystal lattice after the Pb^{2+} emission centre excitation [18]. At this point, the completion of Cs_4PbX_6 luminescence study for the case X = I is highly demanding. Recent results related to the emission of Pb-based aggregated phases in CsI:Pb single crystals have shown rather complex behaviour of observed emission spectra, but the x-ray diffraction spectroscopy failed in finding any Cs–Pb–I ternary structures even after extended annealing procedures [12, 19]. However, ternary Cs–Pb–X microphases seem to be more easily evidenced in co-evaporated CsX–PbX_2 thin films with respect to Pb-doped single crystals due to the higher percentage of PbX_2 component allowed in the thin film samples grown—as shown for X = Br [12, 13].

It is the aim of this paper to describe the creation and the optical properties of Cs–Pb–I ternary microphases in the co-evaporated CsI–PbI_2 thin films.

2. Experiment

The absorption spectra of thin films were measured in UV/VIS spectral range using M40 spectrophotometer modified for low temperature measurements. Luminescence and decay kinetics spectra were measured by Spectrofluorometer 199S (Edinburgh Instrument) equipped by the hydrogen steady-state and coaxial ns pulsed flashlamps (for further description see e.g. [7, 9, 17]). All the spectra were corrected for the experimental distortions and the decay curves in the ns time scale were deconvoluted to extract true decay times as well.

X-ray diffraction (XRD) measurements have been carried out using a Siemens D5000 diffractometer with Cu Kα radiation (λ = 1.5406 Å). In order to obtain higher resolution and an improved full width at half maximum (FWHM) and intensity, we have performed the Bragg–Brentano method using fixed slits. Small grazing incidence angles were used (0.1–2°) in the measurements of diffraction spectra. The interpretation of the XRD spectra is based on the JCPDS database of the structures. In the case of the Cs_4PbI_6 structure good agreement with the observed experimental diffraction spectrum was obtained only after simulation of its diffraction pattern based on Cs_4PbBr_6 reflections. Their change after Br $\rightarrow$ I exchange was derived taking into account the diffraction pattern change from $CsPbBr_3$ to $CsPbI_3$ structures.

Morphology of thin films was investigated by atomic force microscopy (AFM). AFM measurements were performed in contact mode with a Park Scientific Instruments CP microscope equipped with a high aspect ratio conical tip (PSI UltraleverTM with 80° sidewall angle and 5 nm minimum radius).

The samples were obtained by evaporation of $CsPbI_3$ powder (obtained by crushing a $CsPbI_3$ crystal previously grown using the Bridgman technique) from a single crucible (CPI3 sample series) or by co-evaporation of CsI and PbI_2 powders (99.9 + % purity) on quartz and glass substrates using independently driven molybdenum crucibles (CPM3 sample series) under vacuum. The typical growth rate was about 1 nm s^{-1} with the film thickness obtained about 300–600 nm. Each evaporation procedure yields eight samples with sample support

dimension about 10 × 10 mm^2, which were firstly checked by the absorption measurement as for general homogeneity throughout the series. The samples were then distributed for the XRD, AFM and optical measurements.

3. Experimental results

3.1. X-ray diffraction spectroscopy and AFM measurements

The XRD spectrum of the CPM3-2 sample is shown in figure 1. Diffraction peaks related to four different structures were found and they are marked in the figure. The approximate volume percentage of these four phases present in this thin film was estimated from the XRD spectrum as follows: CsI, 75%, Cs_4PbI_6, 15%, $CsPbI_3$, 5% and PbI_2, 5%. The aggregate (crystallite) sizes were determined by the Warren–Averbach method [20] and the medium sizes obtained are as follows: CsI, 43 nm, Cs_4PbI_6, 36 nm, $CsPbI_3$, 24 nm and PbI_2, 34 nm.

A typical AFM picture is shown in figure 2 for the CPM3-3 sample. The method does not allow us to distinguish among the different chemical compounds just mentioned, but it shows that the grain size of a crystallite is between 100 and 300 nm, which is a somewhat higher estimate with respect to the above values obtained from the XRD measurements.

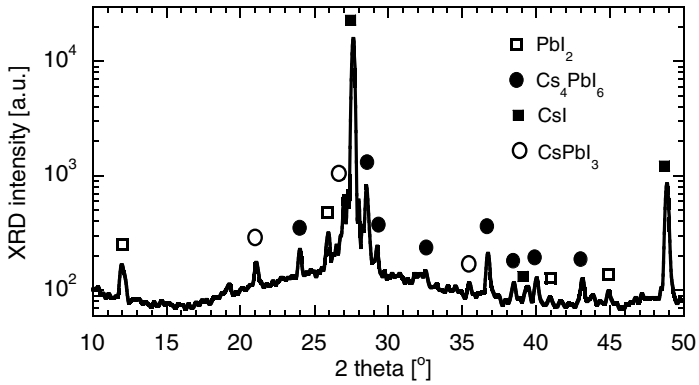

Figure 1. X-ray diffraction pattern of the CPM3-2 thin film at 1° grazing incidence angle.

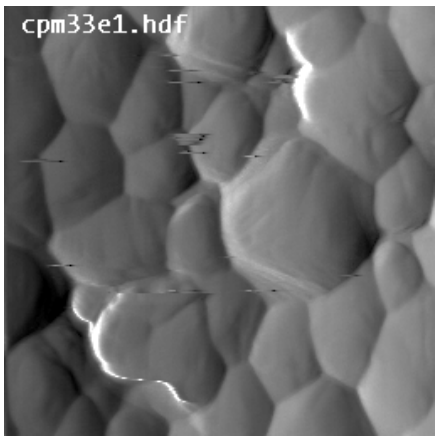

Figure 2. AFM picture of the CPM3-3 sample (1 × 1 μm^2 area) showing the grain morphology of the thin films grown.

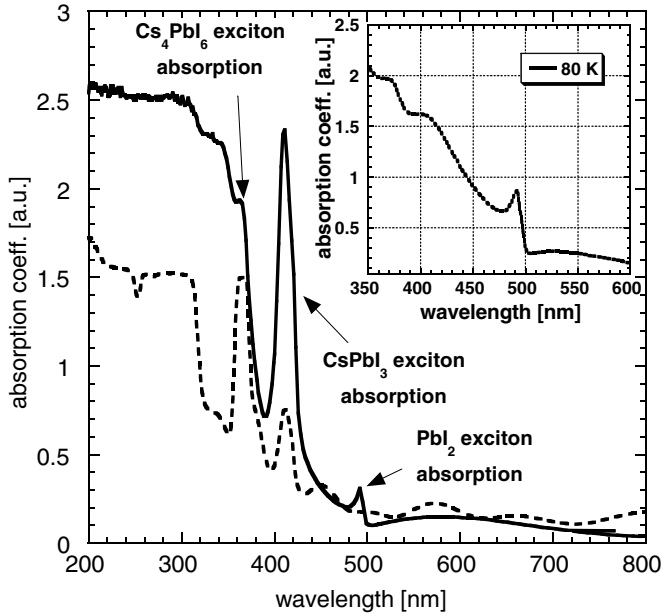

Figure 3. The absorption spectra of the CPI3-2 (continuous line) and CMP3-2 (dashed line) samples at 80 K. In the inset, the absorption of PbI_2 thin film is shown at 80 K.

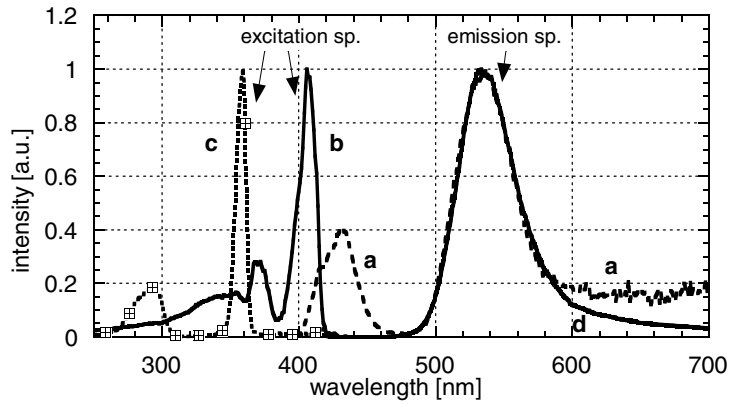

Figure 4. Emission (a) and excitation (b), (c) spectra of the CPI3-2 film at 5 K. (a) exc. = 370 nm; (b) em. = 535 nm; (c) em. = 435 nm. (d) Emission spectrum of the bulk $CsPbI_3$ sample, exc. = 337 nm, $T = 10$ K.

3.2. Absorption spectra

The absorption spectra of the CPI3-2 and CPM3-2 samples at 80 K are shown in figure 3. In the spectrum of the CPI3-2 thin film (higher relative content of Pb ions in the evaporated substance with respect to the CPM3-2 sample) an increased amplitude of 410 nm absorption and another peak at about 490 nm can be noticed. In the inset, PbI_2 thin film absorption is shown at 80 K in the region 350–600 nm. The PbI_2 film was prepared in a similar way as the CPI3 sample series.

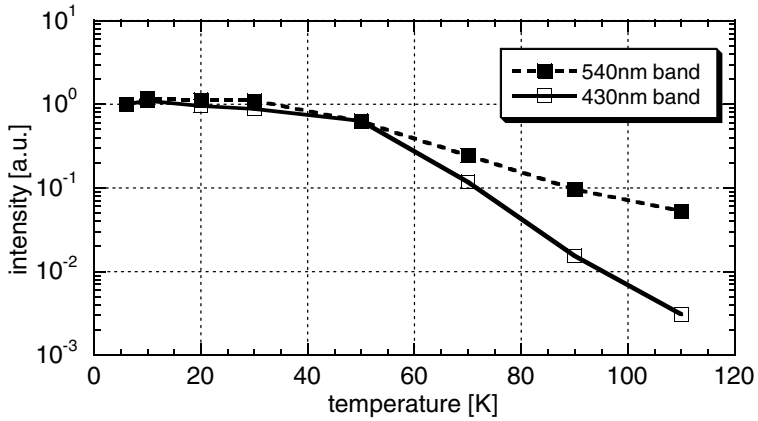

Figure 5. Temperature dependences of the 430 and 535 nm emissions in the CPI3-2 sample excited at 358 nm and 400 nm, respectively.

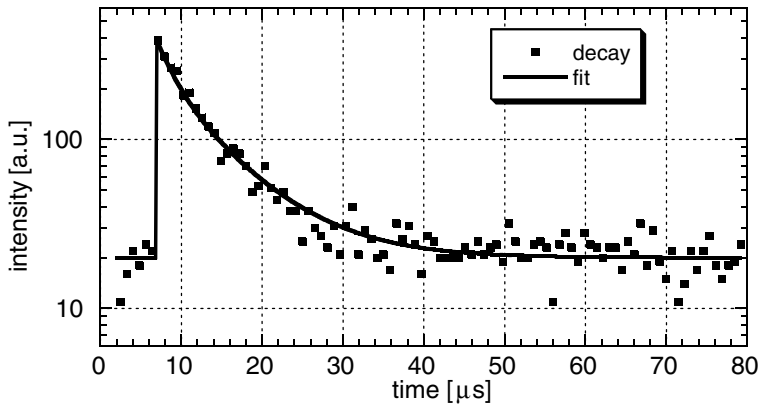

Figure 6. The luminescence decay of the CPI3-2 sample, exc. = 325 nm, em. = 535 nm, $T = 5$ K.

3.3. Luminescence characteristics

In figure 4 the excitation and emission spectra of the CPI3-2 sample are given. Essentially, two luminescent phases can be distinguished: the first one is characterized by a rather smooth excitation spectrum showing a sharp peak round 406 nm and a broad emission band at 535 nm. The second luminescent phase shows a two-peak excitation spectrum (295 and 360 nm) and the emission band round 430 nm. In figure 5 the temperature dependence of the 430 nm and 535 nm emissions is given showing different quenching conditions in the two phases. For the CPM3-2 sample similar spectral characteristics are obtained, but the 535 nm emission band becomes less intense with respect to that at 430 nm (at the same excitation wavelength) in comparison with the CPI3-2 sample. The emission spectrum of the bulk $CsPbI_3$ sample used for CPI3 thin film creation is shown in figure 4, curve d, which shows the 535 nm band again.

Decay kinetics in the 430 and 535 nm bands was measured as well. In figure 6, the decay curve of 535 nm emission is shown at 5 K being approximated by a two-exponential function

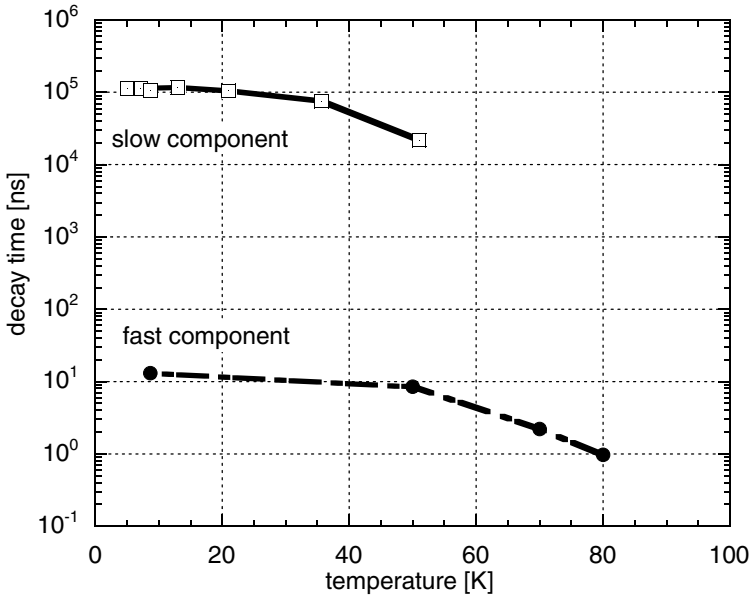

Figure 7. Temperature dependence of the decay times related to the 430 nm emission measured at the CPM3-2 sample, exc. = 358 nm.

$I(t) = 300\exp[-t/2160\text{ ns}] + 370\exp[-t/7680\text{ ns}]$. With increasing temperature the decay becomes much faster ($I(t) = 13\exp[-t/163\text{ ns}]+200\exp[-t/383\text{ ns}]$ at 50 K). Simultaneous decrease of the emission intensity can be noticed in figure 5. No fast components in the ns time scale were detected at the lowest temperatures in the 535 nm band. The 430 nm emission shows two-component behaviour in its decay, which is qualitatively very similar to that reported for Cs_4PbX_6 (X = Cl,Br) [9, 12, 13]. Namely, at 4.2 K the fast and slow components of decay time of about 15 ns and 110 μs, respectively, were detected. The temperature dependence of the fast and slow component decay times is given in figure 7.

4. Discussion

The XRD measurements gave evidence of the $CsPbI_3$ and Cs_4PbI_6 nanoaggregate formation in the thin film samples studied. The disagreement between the grain size determination from XRD and AFM measurement can be explained, if one takes into account the fact that XRD determination is based on the size of defect-free volume, while the AFM measurement visualizes just the grains themselves apart from the degree of their structural (im)perfection. Taking into account the grain (crystallite) sizes obtained from both experiments, it is reasonable to conclude that an average grain observed in AFM contains other smaller crystallites belonging to different orientations, as observed in XRD.

In the ascription of the observed optical features it is worth noting that the single Pb^{2+}-based emission centres in the CsI single crystal matrix show completely different excitation and emission spectra [21] from those reported here. Also the occurrence of such centres is highly improbable due to the high percentage of PbI_2 component in the vapour phase. Thus the observed optical characteristics should be related mostly to the Pb-containing aggregates evidenced by the XRD measurements. The knowledge of the position of the exciton-related

reflection peak in the bulk $CsPbI_3$ in [15] at around 410 nm (4.2 K) is of great advantage. In [15] also an emission band around 530 nm was reported and ascribed to the auto-localized exciton at the Pb^{2+} site. Thus the absorption peak around 410 nm in figure 3, the excitation spectrum under the curve b in figure 4 and the emission band at 535 nm (figure 4, curve a) can be ascribed to the $CsPbI_3$ nanocrystals, which are evidenced by the XRD measurements in figure 1. The absorption peak at 490 nm coincides for the CPI3-2 and PbI_2 thin films in figure 3, so that it apparently belongs to nanocrystalline PbI_2 excitonic transition both in the CPI3-2 and CPM3-2 samples. This interpretation is supported also by PbI_2 optical characterization in the literature [22, 23]. The absorption peak at 360 nm, the excitation spectrum under the curve c in figure 4 and the emission peak at 430 nm can be ascribed to the Cs_4PbI_6 nanocrystals evidenced by XRD measurements in figure 1. This conclusion is supported by (i) similarity in the position of the just mentioned absorption, excitation and emission peaks with KI:Pb [24] (see also the arguments in the introduction); (ii) two component decay qualitatively similar to that of KI:Pb [25] and Cs_4PbX_6 (X = Cl, Br) materials [9, 14]; (iii) correlated increase of the XRD integrated peak intensity (related to Cs_4PbI_6 phase) and of relative height of the absorption peak at 360 nm (with respect to the 406 nm one) within the group of CPI3 and CPM3 samples.

By evaporation of essentially single phase $CsPbI_3$ powder, we have obtained apparently the mixture of both the $CsPbI_3$ and Cs_4PbI_6 phases. This demonstrates the instability of $CsPbI_3$ molecules in the vapour phase and the tendency of the CsI–PbI_2 system to create both the ternary compounds, which are allowed by the phase diagram [16]. This property might be an obstacle in an application based just on one structural phase ($CsPbI_3$ or Cs_4PbI_6) in such a thin film system. Presented data show that the volume ratio of both phases is dependent on the stoichiometry in the vapour phase and the dependence on another technological parameter (e.g. the evaporation rate) is not excluded. This aspect requires further study and is beyond the scope of this paper.

It is worth mentioning that (similarly to KI:Pb) at 4.2 K the slow component of Cs_4PbI_6 significantly deviates from a single exponential course under 360 nm excitation (the mentioned decay time is obtained in the decay tail), while much lower decay distortion and a generally more intense slow component are obtained under 290 nm excitation. However, the decay time value (110 μs at 4.2 K) is much shorter with respect to KI:Pb and Cs_4PbX_6 (X = Cl, Br) structures, which show a few ms decay times at 4.2 K. Such behaviour can be tentatively explained by a more significant admixture of higher excited states (essentially $^3T_{1u}$ level) into the $^3A_{1u}$ excited state of the Pb^{2+} ion. The latter excited state level is directly involved in the slow component radiative transitions. In such a way the luminescent transition $^3A_{1u} \rightarrow {}^1A_{1g}$ might become less forbidden in Cs_4PbI_6. The reason for such a change with respect to the other structures mentioned is not clear, however, and needs further investigation.

Coming back to the $CsPbI_3$ phase, a very essential difference with respect to the $CsPbX_3$ (X = Cl, Br) ones should be emphasized. The $CsPbX_3$ (X = Cl, Br) materials are known as wide-gap semiconductors with direct band gap transitions [6] and pronounced free exciton emission showing subnanosecond decay times and very small Stokes shift (<50 meV) [1–3, 10]. In $CsPbI_3$ we observe most probably the auto-localization of the excitonic state [15] resulting in a broad (and much slower) emission around 535 nm with the Stokes shift of about 0.74 eV. Alternatively, one could consider the localization of the exciton around a defect or even sequential capture of an electron and hole at a defect in the $CsPbI_3$ nanocrystal followed by their radiative recombination. In the latter case, at the lowest temperatures (5 K) such a process should be more efficient under band-to-band excitation (below 400 nm) with respect to the excitation within the exciton absorption band (410 nm). However, it is not observed in the excitation spectrum of 535 nm emission (figure 4, curve b).

5. Conclusion

Ternary $CsPbI_3$ and Cs_4PbI_6 nanophases were demonstrated in the co-evaporated CsI–PbI_2 thin film systems by the XRD measurements. In agreement with the literature data for the bulk $CsPbI_3$, the $CsPbI_3$ nanocrystals show excitonic absorption round 410 nm and a broad-band emission around 535 nm. This emission shows two-exponential decay in the μs time scale at 4.2 K. The absorption at 365 nm was ascribed to the excitonic transition based on the $(PbI_6)^{4-}$ octahedron in the Cs_4PbI_6 nanostructures. A related emission peak is situated at around 430 nm. Two-component decay kinetics was found, which is qualitatively similar to those in the isostructural Cs_4PbX_6 (X = Cl, Br) compounds reported earlier.

Acknowledgment

Financial support of NATO Linkage Grant OUTR.LG 960952 and of NSFC grant No 59672001 is gratefully acknowledged. Thanks are due to Paolo Aloe and to Giovanni Capellini, Department of Physics, Universita Roma Tre for the thin film sample preparation and for performing the AFM measurements, respectively.

References

[1] Amitin L N, Anistratov A T and Kuznetsov A I 1979 *Sov. Phys.–Solid State* **21** 2041
[2] Pashuk I P, Pydzirailo N S and Macko M G 1981 *Sov. Phys.–Solid State* **23** 1263
[3] Nikl M, Mihokova E, Nitsch K, Polak K, Rodova M, Pazzi G P, Fabeni P and Gurioli M 1994 *Chem. Phys. Lett.* **220** 14
[4] Calistru D M, Mihut L, Lefraut S and Baltog I 1997 *J. Appl. Phys.* **82** 5391
[5] Hirotsu S 1972 *Phys. Lett.* A **41** 55
[6] Heidrich K, Kunzel H and Treuch J 1984 *Solid State Commun.* **25** 887
[7] Nikl M, Nitsch K, Polak K, Pazzi G P, Fabeni P, Citrin D S and Gurioli M 1995 *Phys. Rev.* B **51** 5192
[8] Nitsch K, Cihlár A, Dušek M, Hamplová V, Nikl M, Zachová H and Ryšavá N 1993 *Phys. Status Solidi* a **135** 565
[9] Nikl M, Mihóková E and Nitsch K 1992 *Solid State Commun.* **84** 1089
[10] Nitsch K, Hamplová V, Nikl M, Polák K and Rodová M 1996 *Chem. Phys. Lett.* **258** 518
[11] Fabeni P, Pazzi G P, Nikl M, Nitsch K, Scacco A, Somma F, Zazubovich S, Santucci S and Phani A R 1998 *Physics and Chemistry of Luminescent Materials VI (Paris, 1997) (Electrochem. Soc. Proc. **PV 97-29**)* ed C Ronda and T Welker, p 186
[12] Nikl M *et al* 1998 *Excitonic Processes in Condensed Matter (Electrochem. Soc. Proc. **PV 98-25**)* ed R T Williams and W M Yen (Pennington, NJ) p 250
[13] Nikl M *et al* 1999 *Physica* E **4** 323
[14] Nikl M, Mihokova E, Nitsch K, Somma F, Giampaolo C, Pazzi G P, Fabeni P and Zazubovich S 1999 *Chem. Phys. Lett.* **306** 280
[15] Voloshinovskij A S, Mjagkota S V, Pidzyrailo N S and Chapko Z A 1987 *Ukr. Fiz. Zh.* **32** 685 (in Russian)
[16] Il'yasov I I, Chaurskii N I, Barsegov D G and Bergman A G 1967 *Russ. J. Inorg. Chem.* **12** 1163
[17] Polák K, Nikl M and Mihóková E 1992 *J. Lumin.* **54** 189
[18] Gaveau B, Mihóková E, Nikl M, Polák K and Schulman L S 1998 *Phys. Rev.* B **58** 6938
[19] Babin V *et al* 1999 *Radiat. Eff. Defects Solids* **149** 119
[20] Warren E and Averbach B L 1953 *J. Appl. Phys.* **21** 595
[21] Aceves R *et al* 1995 *Inorganic Scintillators and their Applications, Proc. SCINT'95 (Delft, 1995)* ed P Dorenbos and C W van Eijk (Delft University Press) p 445
[22] Watanabe M and Hayashi T 1994 *J. Phys. Soc. Japan* **63** 785
[23] Ping Gu and Watanabe M 1995 *J. Phys. Soc. Japan* **64** 4450
[24] Schmitt K, Sivasankar V S and Jacobs P W M 1982 *J. Lumin.* **27** 313
[25] Mihokova E, Nikl M, Polak K and Nitsch K 1994 *J. Phys.: Condens. Matter* **6** 293